Albumin-fused long-acting FGF21 analogue for the treatment of non-alcoholic fatty liver disease

Mayuko Chikamatsu[a,#], Hiroshi Watanabe[a,#,*], Yuhi Shintani[a], Ryota Murata[a], Masako Miyahisa[a], Ayano Nishinoiri[a], Tadashi Imafuku[a], Mei Takano[a], Nanaka Arimura[a], Kohichi Yamada[a], Miya Kamimura[a], Baki Mukai[a], Takao Satoh[b], Hitoshi Maeda[a], Toru Maruyama[a]

[a]Department of Biopharmaceutics, Graduate School of Pharmaceutical Sciences, Kumamoto University, 5-1 Oe-honmachi, Chuo-ku, Kumamoto 862-0973, Japan.

[b]Kumamoto Industrial Research Institute, Kumamoto, Japan

[#]Chikamatsu and Watanabe contributed equally to this study

[*]Corresponding authors:

Hiroshi Watanabe, Associate Professor

Department of Biopharmaceutics, Graduate School of Pharmaceutical Sciences,

Kumamoto University, 5-1 Oe-honmachi, Chuo-ku, Kumamoto 862-0973, Japan.

Tel.: +81-96-371-4855; Fax: +81-96-362-4855;

E-mail: hnabe@ kumamoto-u.ac.jp

Abstract

Non-alcoholic fatty liver disease (NAFLD) currently affects about 25% of the world's population, and the numbers continue to rise as the number of obese patients increases. However, there are currently no approved treatments for NAFLD. This study reports on the evaluation of the therapeutic effect of a recombinant human serum albumin-fibroblast growth factor 21 analogue fusion protein (HSA-FGF21) on the pathology of NAFLD that was induced by using two high-fat diets (HFD), HFD-60 and STHD-01. The HFD-60-induced NAFLD model mice with obesity, insulin resistance, dyslipidemia and hepatic lipid accumulation were treated with HSA-FGF21 three times per week for 4 weeks starting at 12 weeks after the HFD-60 feeding. The administration of HSA-FGF21 suppressed the increased body weight, improved hyperglycemia, hyperinsulinemia, and showed a decreased accumulation of plasma lipid and hepatic lipid levels. The elevation of C16:0, C18:0 and C18:1 fatty acids in the liver that were observed in the HFD-60 group was recovered by the HSA-FGF21 administration. The increased expression levels of the hepatic fatty acid uptake receptor (CD36) and fatty acid synthase (SREBP-1c, FAS, SCD-1, Elovl6) were also suppressed. In adipose tissue, HSA-FGF21 caused an improved adipocyte hypertrophy, a decrease in the levels of inflammatory cytokines and induced the expression of adiponectin and thermogenic factors. The administration of HSA-FGF21 to the STHD-01-induced NAFLD model mice resulted in suppressed plasma ALT and AST levels, oxidative stress, inflammatory cell infiltration and fibrosis. Together, HSA-FGF21 has some potential for use as a therapeutic agent for the treatment of NAFLD.

KEYWORDS: Albumin fusion; FGF21; Non-alcoholic fatty liver disease; Non-alcoholic steatohepatitis; Fatty acid: Insulin resistance

1. Introduction

Non-alcoholic fatty liver disease (NAFLD) is a condition in which an excessive intake of energy results in the accumulation of triglycerides in the liver. It is classified as either non-alcoholic fatty liver (NAFL) and non-alcoholic steatohepatitis (NASH). NASH is a progressive disease with a high risk of progressing to cirrhosis and cancer, and about 20% of NAFLD patients have NASH. NAFLD currently affects about 25% of the world's population[1], and this number continues to rise as the number of obese patients increases. By 2030, NASH-induced liver failure is expected to be the leading cause of liver transplantation[1-3]. However, there are currently no approved treatments for NAFLD/NASH.

NAFLD/NASH is regarded as a type of metabolic syndrome, and many patients have obesity, type 2 diabetes and dyslipidemia as underlying diseases[1, 4]. Insulin resistance is a particularly important risk factor, and NAFLD patients with insulin resistance eventually develop NASH which, in turn, is a high risk factor for progression to end-stage liver failure and a high mortality rate[5-8]. The pathophysiology of NAFLD is complicated due to the variety of pathophysiological backgrounds of these subjects. The "multiple parallel hits hypothesis" proposed by Tilg et al. is widely recognized as the mechanism responsible for the progression of this disease[9]. In this hypothesis, which is based on obesity and insulin resistance, the pathogenesis is thought to occur through the simultaneous interaction of a number of factors that include fat accumulation in hepatocytes, the abnormal secretion of adipokines, the production of inflammatory cytokines derived from immune cells and oxidative stress. Therefore, therapeutic drugs against NAFLD/NASH should be able to target the above multiple disease progression factors.

Fibroblast growth factor 21 (FGF21) is a hormone-like protein with a molecular weight of 19.5 kDa that belongs to the FGF family of proteins and is produced by liver, adipose tissue,

muscle and pancreas. Serum levels of FGF21 are elevated in obesity, type 2 diabetes and NAFLD/NASH[10, 11]. In the case of NAFLD, serum FGF21 levels increases with the progression of the disease[12]. On the other hand, it was reported that the pharmacological administration of FGF21 to obesity model mice, type 2 diabetes model mice and monkeys showed hypoglycemic effects, improved insulin sensitivity, the reduction of serum triglycerides and cholesterol, which lead to weight loss and an improved fatty liver[13-15]). Furthermore, it also reported that FGF21 has pleiotropic pharmacological effects such as enhanced heat production in adipose tissue and the induction of adiponectin[16-19]. Given these observations, FGF21 would be expected to be a novel and unique therapeutic agent that can comprehensively improve the overall pathology associated with NAFLD.

However, since the recombinant wild type FGF21 was unstable and the plasma half-life was very short due to its low molecular weight, wild type FGF21 itself could not be allowed for clinical application. In fact, the stabilized FGF21[20] and several long-acting FGF21 such as FGF21 molecule linked to a humanized immunoglobulin[21] or polyethylene glycol[22] in addition to Fc-fusion type[23] have been developed so far. We recently successfully generated a long-acting recombinant FGF21 analogue, in which the stabilized mutant FGF21 (ΔHPIP, P171G, A180E, L118C-A134C, S167A) was fused with human serum albumin (HSA) (HSA-FGF21) *via* a polypeptide linker (GGGGSGGGGS), then expressed using a *Pichia* expression system[24]. We also reported that HSA-FGF21 exerts a sustained hypoglycemic effect without causing hypoglycemia in streptozotocin-induced type 1 diabetes model mice[24]. These findings suggested that HSA-FGF21 could also be effective for the treatment of NAFLD/NASH.

In this study, we report on the first pharmacological evaluation of HSA-FGF21 for the treatment of the pathology associated with NAFLD/NASH. Considering the diversity of NAFLD pathology models, we selected two high-fat diet (HFD)-induced NAFLD model mice, HFD-60

and STHD-01.

2.Material & Methods

2.1. Preparation of HSA-FGF21 analogue fusion

The HSA-FGF21 analogue was expressed using *Pichia* expression system. The preparation of HSA-FGF21 analogue fusion was reported in a previous study[24].

2.2. HFD-60-induced NAFLD model mice and the drug administration schedule

C57BL/6J mice (3-week-old, male) purchased from Japan SLC, Inc. (Shizuoka, Japan) were preliminarily housed for 1 week and used as 4-week-old mice. Basal diet CE-2 (CLEA Japan, Inc., Tokyo, Japan) as a normal diet (ND) and HFD-60 (Oriental Yeast Co., Ltd. Tokyo, Japan) as a high-fat diet (HFD) were bred ad libitum for 16 weeks. At 12 weeks after the HFD-60 feeding, PBS (10 mL/kg) or HSA-FGF21 (250, 500 nmol/kg) was administered via the tail vein three times a week. After 4 weeks, the mice were euthanized and evaluated. At the start of the HFD-60 feeding, body weight was used to randomize the normal diet (ND) group and the HFD-60 feeding group, and at 12 weeks after HFD-60 feeding, the HFD-60 feeding group was divided into the PBS group and the HSA-FGF21 (250 or 500 nmol/kg) group based on body weight and blood glucose levels.

2.3. STHD-01-induced NAFLD/NASH model mice and the drug administration schedule

C57BL/6J mice (8-week-old, male) purchased from Japan SLC, Inc. (Shizuoka, Japan) were preliminarily housed for 1 week and used as 9-week-old mice. STHD-01 was donated by EA Pharma Co., Ltd. (Tokyo, Japan). Basal diet CE-2 (CLEA Japan, Inc., Tokyo, Japan) as a ND and STHD-01 (Oriental Yeast Co., Ltd. Tokyo, Japan) as a HFD were fed ad libitum for 4 weeks. Two weeks after the start of the STHD-01 feeding, PBS (10 mL/kg) or HSA-FGF21 (250, 500 nmol/kg) was administered via the tail vein three times a week. Telmisartan (5 mg/kg: Tokyo Kasei, Tokyo, Japan) was orally administered daily for 2 weeks.

2.4. Measurement of plasma biochemical parameters

Plasma lipid concentrations were measured using a Fuji Dry Chem 7000Z (FUJIFILM Tokyo, Japan) and Fuji Dry Chem Slide TG-PIII and TCHO-PIII. Transaminase C-II Test Wako (FUJIFILM Wako Pure Chemical, Tokyo, Japan) was used to measure ALT and AST.

2.5. Measurement of plasma leptin, insulin and adiponectin levels

ELISA kits (LBIS Mouse Insulin and LBIS Leptin-Mouse: FUJIFILM Wako Shibayagi, Tokyo, Japan, Mouse/Rat Adiponectin ELISA Kit: Otsuka Pharmaceutical Co., Ltd. Japan) were used and performed according to the attached protocol.

2.6. Measurement of blood glucose level

In the case of the HFD-60-induced NAFLD model mice, a self-monitoring blood glucose meter Glutest NEO Super (Sanwa Chemical Co., Ltd.) was used. Using a Glutest NEO sensor (Sanwa Chemical Co., Ltd.) as a dedicated sensor, the tip of the tail of the mouse was cut and measured. Fasting blood glucose levels were measured after a 12 hour period of fasting. In the study of STHD-01-induced NASH model mice, a glucose CII-Test Wako (FUJIFILM Wako Pure Chemical Industries, Ltd.) was used.

2.7. Oral glucose tolerance test

After fasting for 12 hours, the mice were given a glucose solution (2 g/kg body weight) and blood glucose levels were measured after 0, 15, 30, 60 and 120 minutes. The glucose solution was prepared by diluting D-(+)-glucose with saline, filter sterilizing, and allowing it to stand at room temperature overnight.

2.8. Oil Red O staining

An Oil Red O staining solution was prepared by adding 0.3 g of Oil Red O powder (FUJIFILM Wako Pure Chemical Industries, Ltd.) to 100 mL of 99% isopropanol followed by incubating at 60°C (6 hours). Frozen liver sections were stained with an Oil Red O staining solution for 15 min and washed with deionized water for 5 min. The sample was then stained with Mayer's hematoxylin solution for 3 minutes, washed with ion-exchanged water for 5 minutes, mounted with a water-soluble mounting medium, Mount-Quick “Aqueous” (Daido Sangyo Co., Ltd., Tokyo, Japan). Images and analysis were performed using a Keyence BZ-X710 microscope (Keyence, Osaka, Japan).

2.9. HE staining

HE staining was performed as described in our previous study[24].

2.10. Determination of hepatic triglycerides (TG) and total cholesterol (TCHO)

After collecting the liver from the mouse, 0.5 mL of methanol was added to about 150 mg of the liver and the sample was then homogenized. The homogenate was mixed with 1 mL of chloroform, 1 mL of 0.9% saline was added, and the suspension was centrifuged (2,800 rpm, 10 min, 4°C). After collecting the lower layer in the vial, it was placed in a block incubator at 55 °C for about 8 hours to allow the solvent to evaporate and to concentrate the sample. Samples were resuspended in 1% Triton X/isopropanol and measured with a Triglyceride E Test Wako and Cholesterol E Test Wako (FUJIFILM Wako Pure Chemical Industries, Ltd.).

2.11. Measurement of various mRNA expression levels by a quantitative RT-PCR method

Measurement of various mRNA expression levels was performed according to our previous

study[24]. The primers used are listed in the Supplemental Table 1.

2.12. Western blotting and enzyme immunostaining

Western blotting and enzyme immunostaining were performed according to our previous study [24]. The antibodies used are listed in the Supplemental Table 2.

2.13. Measurement of fatty acid composition by gas chromatography-mass spectrometry (GC-MS)

Measurement of fatty acid composition by GC-MS was performed as described in our previous study[25].

2.14. Picro-Sirius Red staining

After removing the paraffin attached to the prepared paraffin section by treatment with xylene and ethanol, the sample was stained with iron hematoxylin, washed with water, and stained with a Picro-Sirius red solution. Stained sections were observed under an optical microscope (BZ-X710, Keyence). 10-12 fields were randomly selected from each section and quantified using BZ-Analyzer software

2.15. Culture and differentiation of mouse fibroblast cell line (3T3L1)

Subculture medium was prepared by adding 10 % calf serum, 0.1 mg/mL streptomycin, 100 U/mL penicillin to DMEM (low glucose). The base medium was prepared by adding 10% FBS, 0.1 mg/mL streptomycin, and 100 U/mL penicillin to the DMEM (high glucose). The differentiation medium was prepared by adding 2.5 μM dexamethasone, 500 μM isobutylmethylxanthine, and 10 μg/mL insulin to the basal medium. The maturation-promoting medium was prepared by

adding a 10 μg/mL solution of insulin to the basal medium. 3T3L1 was cultured in subculture medium and used as preadipocytes. After inoculating the plate, it was cultured in subculture medium until it reached confluence. After 24 hours, the medium was replaced with differentiation medium. After inducing differentiation for 48 hours, the medium was replaced with a maturation-promoting medium and cultured for 12 days to obtain mature adipocytes.

2.16. Examination of adiponectin induction ability using 3T3L1 cells

3T3L1 cells were seeded in a 12-well plate at 2.0×10^5 cells/well and differentiated into mature adipocytes. After starvation for 4 hours, PBS, HSA (10, 100 nM), HSA-FGF21 (10-100 nM) and FGF21 (10 nM) were added, RNA extraction was then performed 12 hours later.

2.17. Statistical analyses

All experimental data are shown as the mean±standard error. GraphPad Prism 9 (GraphPad Software, CA) was used as statistical analysis software. The means for more than two groups were compared by one-way ANOVA, and multiple comparison test was performed by the Turkey method. A probability value of $P<0.05$ were considered to be significant.

3. Results

3-1. Therapeutic effect of HSA-FGF21 on obesity

Therapeutic effect of HSA-FGF-21 on obesity was evaluated using NAFLD model mice. Considering the pathological background of NAFLD/NASH patients, we used high-fat diet (HFD)-60-induced NAFLD model mice with obesity and abnormal glucose and lipid metabolism. After 12 weeks of HFD-60 feeding, PBS (10 mL/kg, *i.v.*) or HSA-FGF21 (250, 500 nmol/kg, *i.v.*) was administered three times a week for 4 weeks (Fig. 1A). In the 12th week of HFD-60 feeding, randomization was performed by body weight and blood glucose level. The HFD-60 feeding caused a gradual increase in body weight, and after 12 weeks, a difference of about 15 g was observed compared to the normal diet (ND) group (Fig. S1A). In the HSA-FGF21 administration group, body weight gain was suppressed (Fig. 1B and C). Body weight was significantly decreased from 20 days after administration in the 500 nmol/kg group, and from 25 days after administration in the 250 nmol/kg group (Fig. 1C). In addition, HFD-60 feeding significantly increased the weight of epididymal white adipose tissue (eWAT), mesenteric white adipose tissue (mWAT), inguinal subcutaneous white adipose tissue (ingWAT) and interscapular brown adipose tissue (iBAT) (Fig. 1D-H). At this time, eWAT, ingWAT, and iBAT had all been observed to have accumulated lipid droplets by HE staining (Fig. S1B). On the other hand, the administration of HSA-FGF21 (250, 500 nmol/kg) reduced this accumulation (Fig. S1B) and suppressed the weight of adipose tissues that had been induced by HFD-60 (Fig. 1D-H,). Food intake was slightly increased in the HSA-FGF21 (250, 500 nmol/kg) administration group compared to the ND group and the PBS administration group (Fig. S1C), indicating that the effects of HSA-FGF21 was independent of food intake. The administration of HSA-FGF21 suppressed the elevation in plasma leptin levels associated with obesity (Fig. S1D). These data suggest that HSA-FGF21 ameliorates the obesity induced by feeding HFD-60.

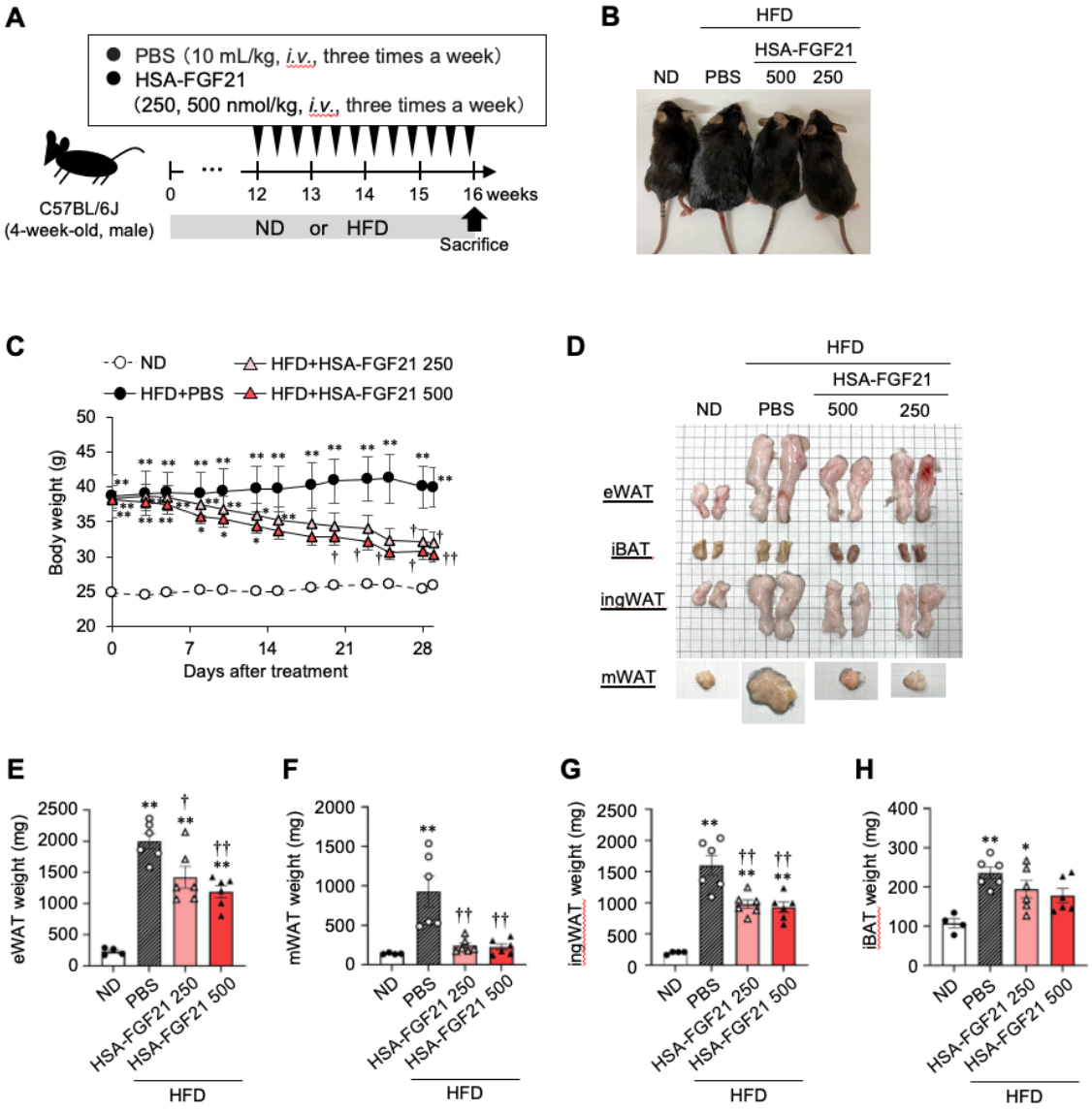
A
PBS (10 mL/kg, i.v., three times a week)
HSA-FGF21
(250, 500 nmol/kg, i.v., three times a week)
C57BL/6J
(4-week-old, male)
0
12
13
14
15
16 weeks
ND or HFD
Sacrifice
B
HFD
HSA-FGF21
ND
PBS
500
250
C
ND
HFD+PBS
HFD+HSA-FGF21 250
HFD+HSA-FGF21 500
Body weight (g)
Days after treatment
D
HFD
HSA-FGF21
ND
PBS
500
250
eWAT
iBAT
ingWAT
mWAT
E
eWAT weight (mg)
F
mWAT weight (mg)
G
ingWAT weight (mg)
H
iBAT weight (mg)
ND
PBS
HSA-FGF21 250
HSA-FGF21 500
HFD

Figure 1. Effect of HSA-FGF21 on obesity

(A) Experimental procedure for evaluating the therapeutic effect of HSA-FGF21 on HFD-60-induced NAFLD model mice: C57BL/6J mice (4-week-old, male) were fed a normal diet (ND) or high fat diet (HFD-60). Mice were randomized at 12 weeks of HFD-60 feeding, and PBS (10 mL/kg) or HSA-FGF21 (250, 500 nmol/kg) were administered intravenously three times a week for 4 weeks. (B) Representative image of mice from each group at 4 weeks after the administration of PBS or HSA-FGF21. (C) Body weight was monitored during the 4 week treatment. (D) Representative images of adipose tissues harvested from mice after the treatment. Weight of (E) eWAT, (F) mWAT, (G) ingWAT and (H) iBAT of mice at 4 weeks after the administration of HSA-FGF21. Results are the means±S.E. (n=4-6). $^{*}p<0.05$, $^{**}p<0.01$ compared with ND group, $^{\dagger}p<0.05$, $^{\dagger\dagger}p<0.01$ compared with PBS-treated HFD-60 group.

3-2. Therapeutic effect of HSA-FGF21 on glucose metabolism and dyslipidemia

We also investigated the therapeutic effect of HSA-FGF21 on abnormal glucose metabolism. Fasting blood glucose levels and plasma insulin concentrations were measured on day 25 after the administration of PBS or HSA-FGF21. As a result, the elevated fasting blood glucose level and plasma insulin concentration in the PBS-treated group were both reduced by the administration of HSA-FGF21 (250, 500 nmol/kg) (Fig. 2A, B). In order to evaluate the effect of HSA-FGF21 on glucose tolerance, an oral glucose tolerance test (OGTT) was performed at 25 days after the administration of HSA-FGF21 (Fig. 2C). Compared with the PBS-administered group, the blood glucose levels were significantly decreased in the HSA-FGF21 (250, 500 nmol/kg)-administered group after glucose loading, suggesting that HSA-FGF21 improves glucose tolerance. As an evaluation of insulin resistance, the level of phosphorylated Akt in the liver was evaluated by Western-blotting. As a result, the levels of phosphorylated Akt increased in the HSA-FGF21 (250, 500 nmol/kg) administration group, suggesting that insulin signaling by HSA-FGF21 had been enhanced (Fig. S2A). The expression of GLUT4 mRNA in eWAT and ingWAT was also determined. The decreased GLUT4 mRNA expression tended to recover to the

same level as the ND group (Fig. S2B and C). These data suggest that HSA-FGF21 improved insulin sensitivity followed by improving glucose metabolism.

We next evaluated the effect of HSA-FGF-21 on dyslipidemia. Plasma triglyceride (TG) and total cholesterol (TCHO) levels, which were markedly increased in the PBS-treated group, were both significantly reduced by the administration of HSA-FGF21 (250, 500 nmol/kg) (Fig. 2D, E). This finding indicates that HSA-FGF21 is capable of ameliorating the dyslipidemia that was induced by feeding HFD-60.

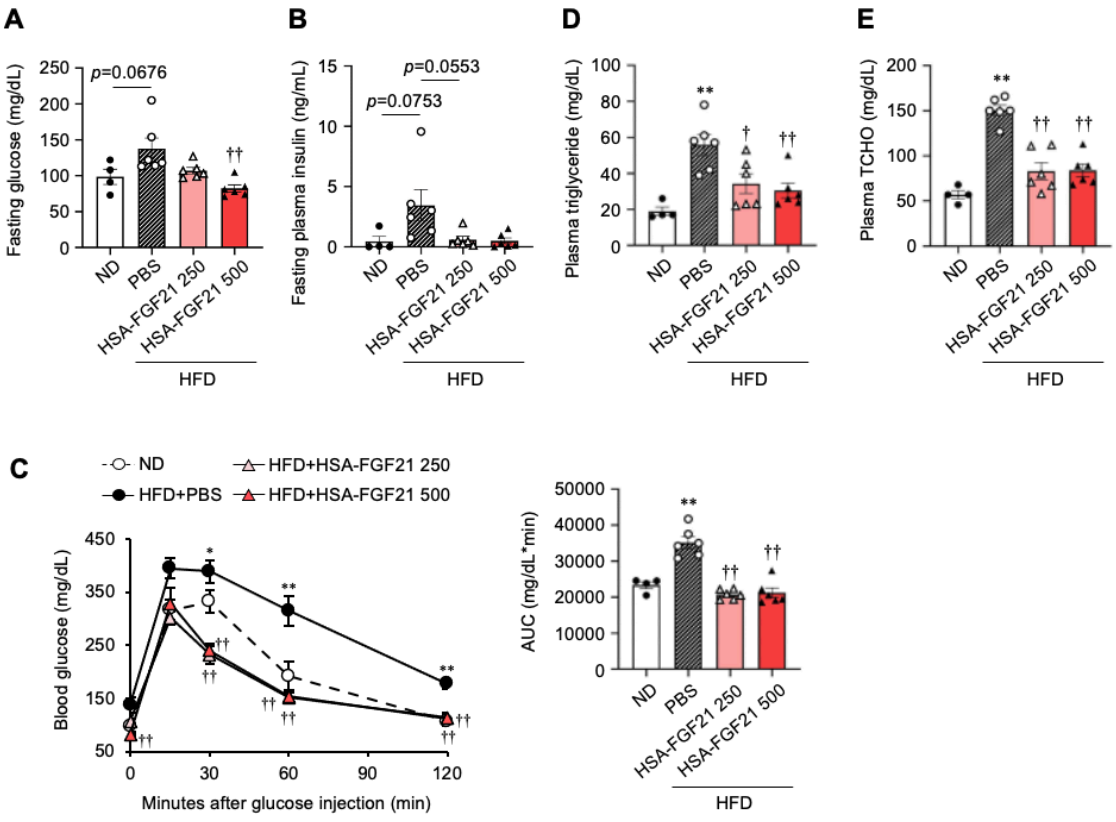

Figure 2. Effect of HSA-FGF21 on glucose metabolism and dyslipidemia

Fasting (A) blood glucose and (B) plasma insulin levels of mice fasted for 12 hours were measured at day 25 after the administration of HSA-FGF21. (C) OGTT was performed at day 25 after the administration of HSA-FGF21. Mice were fasted for 12 hours prior to an oral administration of D-glucose (2 g/kg). Blood glucose levels were measured at 0, 15, 30, 60 and 120 mins after glucose injection. (D) Plasma triglyceride levels and (E) total cholesterol levels were measured at 4 weeks after the administration of HSA-FGF21. Results are the mean±S.E. (n=4-6). $^{*}p<0.05$, $^{**}p<0.01$ compared with ND group, $^{\dagger}p<0.05$, $^{\dagger\dagger}p<0.01$ compared with PBS-treated HFD-60 group.

3.3 Therapeutic effect of HSA-FGF21 on hepatic steatosis and liver injury

We next evaluated the accumulation of lipid in the liver. In the PBS-administered group, the liver showed whitening due to the accumulation of excess fat, and this color change was improved by the administration of HSA-FGF21 (250, 500 nmol/kg) (Fig. 3A upper panels). Liver weight tended to increase in the PBS-administered group, but it was significantly decreased in the HSA-FGF21 (250, 500 nmol/kg)-administered group (Fig. 3B). Histological evaluation of liver tissue revealed that extensive vesicular and macrovesicular cellular vacuoles, lipid droplets and fat infiltration into hepatocytes were observed in the PBS-administered group, whereas the HSA-FGF21 (250, 500 nmol/kg) administered group showed less lipid droplets and the infiltration of fat into the liver was decreased (Fig. 3A middle and lower panels). Reflecting these histological findings, the amount of TG in the liver was significantly increased in the PBS-administered group, whereas the administration of HSA-FGF21 (250, 500 nmol/kg) resulted in the TG levels being decreased to the same level as that for the ND group (Fig. 3C). TCHO levels in the liver and plasma ALT or AST levels showed a similar tendency to the TG levels (Fig. 3D~E).

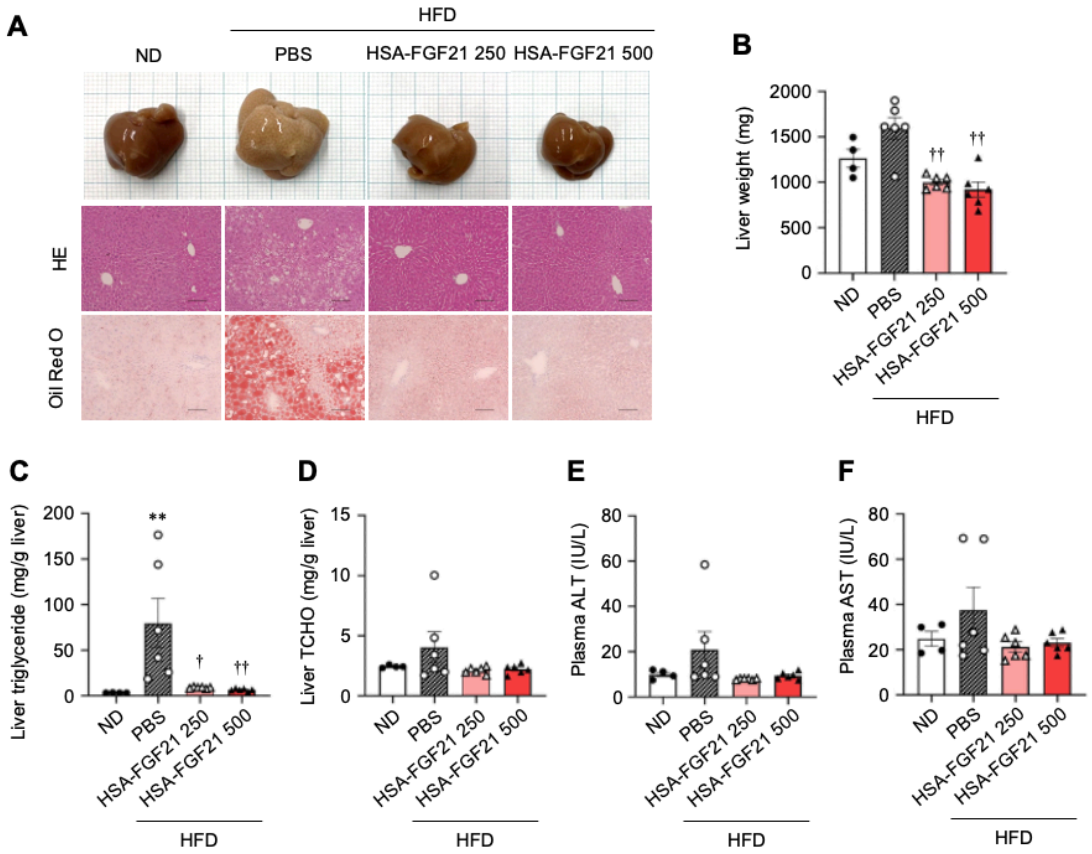

Figure 3. Effect of HSA-FGF21 on hepatic steatosis and liver injury

(A) Representative liver tissues that were harvested from mice at 4 weeks after the administration of HSA-FGF21. Representative photomicrographs of hematoxylin and eosin (HE) and Oil red O stained liver sections at 4 weeks after the administration of HSA-FGF21 are shown. Original magnification: ×200. Scale bars represent 100 μm. (B) Liver weight of mice at 4 weeks after the administration of HSA-FGF21. (C) Hepatic TG and (D) TCHO levels were measured at 4 weeks after the administration of HSA-FGF21. Plasma (E) ALT and (F) AST levels were measured at 4 weeks after the administration of HSA-FGF21. Results are the mean±S.E. (n=4-6). $^{**}p<0.01$ compared with ND group, $^{\dagger}p<0.05$, $^{\dagger\dagger}p<0.01$ compared with PBS-treated HFD-60 group.

3.4 Changes in hepatic fatty acids composition by HSA-FGF21

It was recently reported that changes in the fatty acid content in the liver contribute to the

exacerbation of NAFLD/NASH and insulin resistance[26-29]. To address this issue, we extracted the total lipids in the liver and measured the content of the individual fatty acids using gas chromatograph-mass spectrometry (GC-MS). In the case of the PBS-treated group, C16:0 (palmitic acid) and C18:0 (stearic acid), which are involved in the induction of oxidative stress and inflammation[30, 31], C18:1 (oleic acid), which accumulates as lipids[32] and C18:2 (linoleic acid) were all significantly increased (Fig. 4A). The administration of HSA-FGF21 (250, 500 nmol/kg) suppressed these increases in C16:0, C18:0, C18:1 and C18:2 levels.

3.5 Improvement mechanism of HSA-FGF21 on hepatic lipid accumulation

We next investigated the mechanism by which HSA-FGF21 prevents lipid accumulation in the liver. There are mainly four pathways involved in the accumulation of lipid in the liver: 1) fatty acid uptake, 2) fatty acid synthesis, 3) fatty acids β-oxidation, and 4) the excretion of lipids from the liver into the blood[33]. To examine these possibilities, we evaluated the effects of HSA-FGF21 on these four pathways. We initially evaluated the fatty acid uptake pathway. CD36, a scavenger receptor, is involved in fatty acid uptake in the liver, and it has been reported that the expression of CD36 increases with the progression of NAFLD/NASH pathology, thus contributing to the exacerbation of the pathology[34, 35]. Regarding CD36 mRNA expression in the liver, the expression was found to be significantly elevated in the PBS-administered group, and was significantly suppressed by HSA-FGF21 (250, 500 nmol/kg) (Fig. 4B). We next evaluated the fatty acid synthesis pathway. We measured the mRNA expression level of fatty acid synthase (SREBP-1c, FAS, SCD-1, Elovl6) in the liver. The findings indicate that the expression of these molecules tended to increase in the PBS-administered group but that HSA-FGF21 administration suppressed these expression levels (Fig. 4C). We also evaluated the fatty acid β-oxidation pathway. Concerning the level of phosphorylation of AMPK in the liver, no significant

change was observed in any group (Fig. 4D). Similarly, no significant changes were observed in the mRNA expression levels of AMPK downstream factors (PPARα, CPT-1a), but CPT-1a tended to decrease with the administration of HSA-FGF21 (250, 500 nmol/kg) (Fig. 4E). Finally, we evaluated the lipid excretion pathway. Activation of the lipid excretion pathway was evaluated by measuring the level of expression of microsomal triglyceride transport protein (MTP) mRNA in the liver. There was no significant change in the expression of MTP in any group (Fig. 4F). These data suggest that HSA-FGF21 suppressed hepatic lipid accumulation by suppressing fatty acid influx and excessive fatty acid synthesis in the liver.

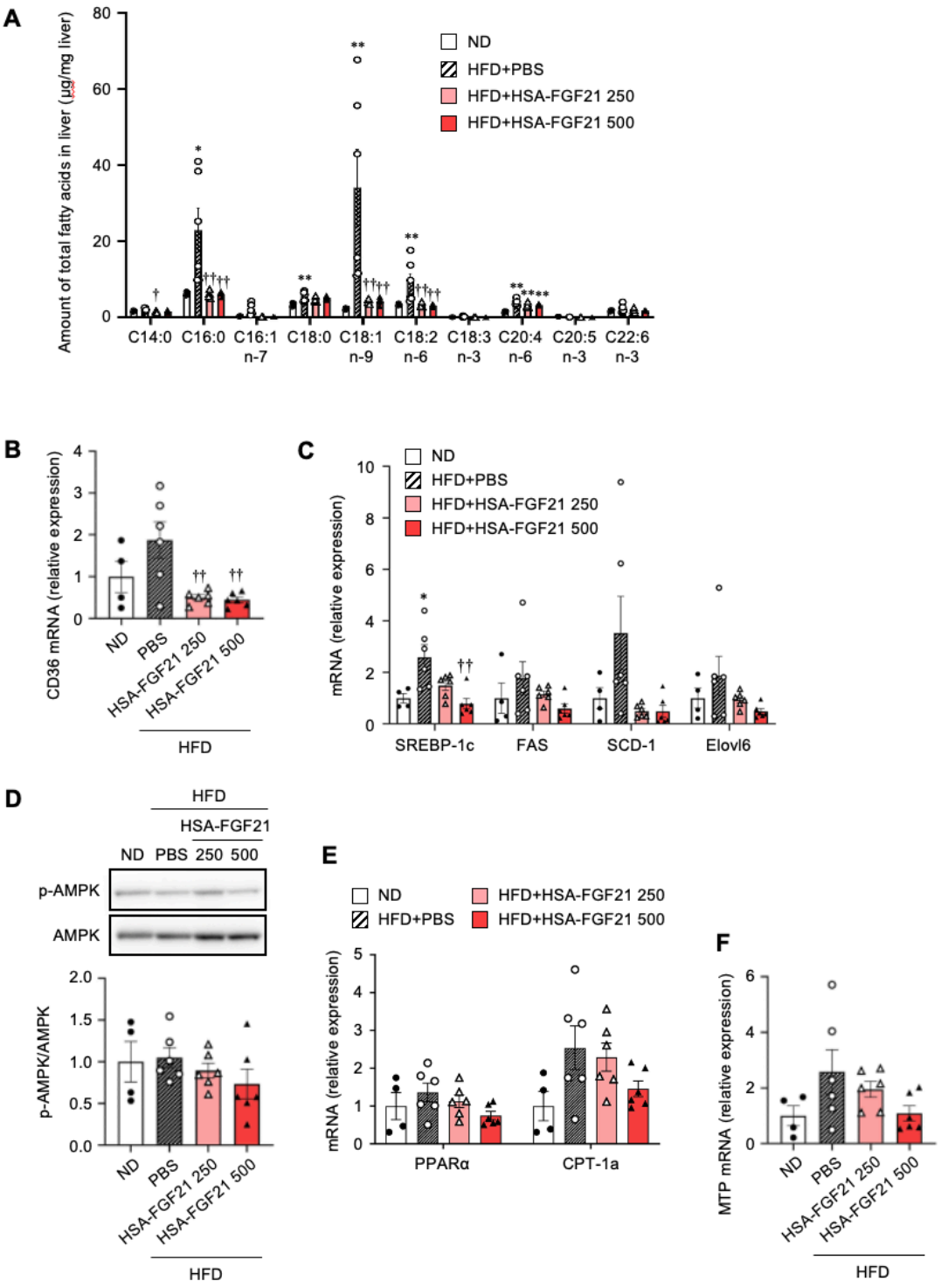
A
Amount of total fatty acids in liver (μg/mg liver)
ND
HFD+PBS
HFD+HSA-FGF21 250
HFD+HSA-FGF21 500
C14:0
C16:0
C16:1 n-7
C18:0
C18:1 n-9
C18:2 n-6
C18:3 n-3
C20:4 n-6
C20:5 n-3
C22:6 n-3
B
CD36 mRNA (relative expression)
ND
PBS
HSA-FGF21 250
HSA-FGF21 500
HFD
C
mRNA (relative expression)
SREBP-1c
FAS
SCD-1
Elovl6
D
HFD
HSA-FGF21
ND PBS 250 500
p-AMPK
AMPK
p-AMPK/AMPK
E
PPARα
CPT-1a
F
MTP mRNA (relative expression)

Figure 4. Effect of HSA-FGF21 on fatty acids composition and genes expression related to hepatic lipid accumulation

(A) Hepatic fatty acid composition was determined using GC-MS at 4 weeks after the administration of HSA-FGF21. (B) Lipid uptake-related gene (CD36) and (C) lipid synthesis-related genes (SREBP-1c, FAS, SCD-1, Elovl6) mRNA expression in liver were determined by quantitative RT-PCR. (D) Western blot analysis of AMPK protein and phosphorylated AMPK in the liver, and (E) fatty acid oxidation-related genes (PPARα, CPT-1a) and (F) lipid efflux-related gene (MTP) mRNA expression in liver were determined at 4 weeks after the administration of HSA-FGF21. Results are the mean±S.E. (n=4-6). $^{*}p<0.05$, $^{**}p<0.01$ compared with ND group, $^{\dagger}p<0.05$, $^{\dagger\dagger}p<0.01$ compared with PBS-treated HFD-60 group.

3.6 Effect of HSA-FGF21 on adipose tissue

Since FGFR1c, the receptor for FGF21, is expressed at very low levels in hepatocytes[36], it is unlikely that FGF21 acts directly on the liver[37], and is thought to exert its effects indirectly through the actions on other organs.

Adipose tissue stores excess energy in the body in the form of TG, and when energy is insufficient, TG molecules are converted into free fatty acids and supply energy to the whole body, thereby regulating the energy in the body. Adipose tissue also functions as the largest endocrine organ in the body, secreting a variety of physiologically active substances called adipokines[38]. It is known that FGF21 acts on adipose tissue where it then suppresses hepatic lipid accumulation and insulin resistance through the induction of adiponectin, which functions to improve glucose and lipid metabolism[19]. In fact, an increase in plasma adiponectin concentration was observed 4 weeks after HSA-FGF21 administration (Fig. 5A). Next, HSA-FGF21 was added to differentiated 3T3L1 adipocytes *in vitro*, and the adiponectin mRNA expression level was measured. As a result, the addition of HSA had no effect on adiponectin expression level, but the addition of HSA-FGF21 increased the mRNA expression level and this increase was

concentration-dependent. In addition, FGF21 was confirmed to induce the same level of expression as HSA-FGF21 at a concentration of about 1/6 that of HSA-FGF21 (Fig. 5B). This indicates that HSA-FGF21 retains the ability to induce the formation of adiponectin that is derived from FGF21.

Adipose tissues include white adipocytes that store energy in the form of TG, while brown and beige adipocytes consume energy as heat. BAT and beige adipose tissue have attracted interest as therapeutic targets for the treatment of obesity-related diseases. It has been reported that the activation of BAT and ingWAT by continuous cold stimulation, and the induction of thermogenic factors in WAT increase energy consumption throughout the entire body, and improve obesity, abnormal glucose metabolism and fatty liver[39, 40]. FGF21 is known to promote energy expenditure by increasing the expression of thermogenic factors in adipose tissues [16]. Therefore, to investigate the issue of whether HSA-FGF21 has the same effect, we determined the mRNA expression levels of thermogenic factors (UCP1, PGC-1α, CPT-1a) in ingWAT, a major thermogenic tissue. As a result, the administration of HSA-FGF21 (250, 500 nmol/kg) caused an increase in the expression of all thermogenic factors (Fig. 5C-E). A similar effect was also found in eWAT and iBAT (Fig. S3).

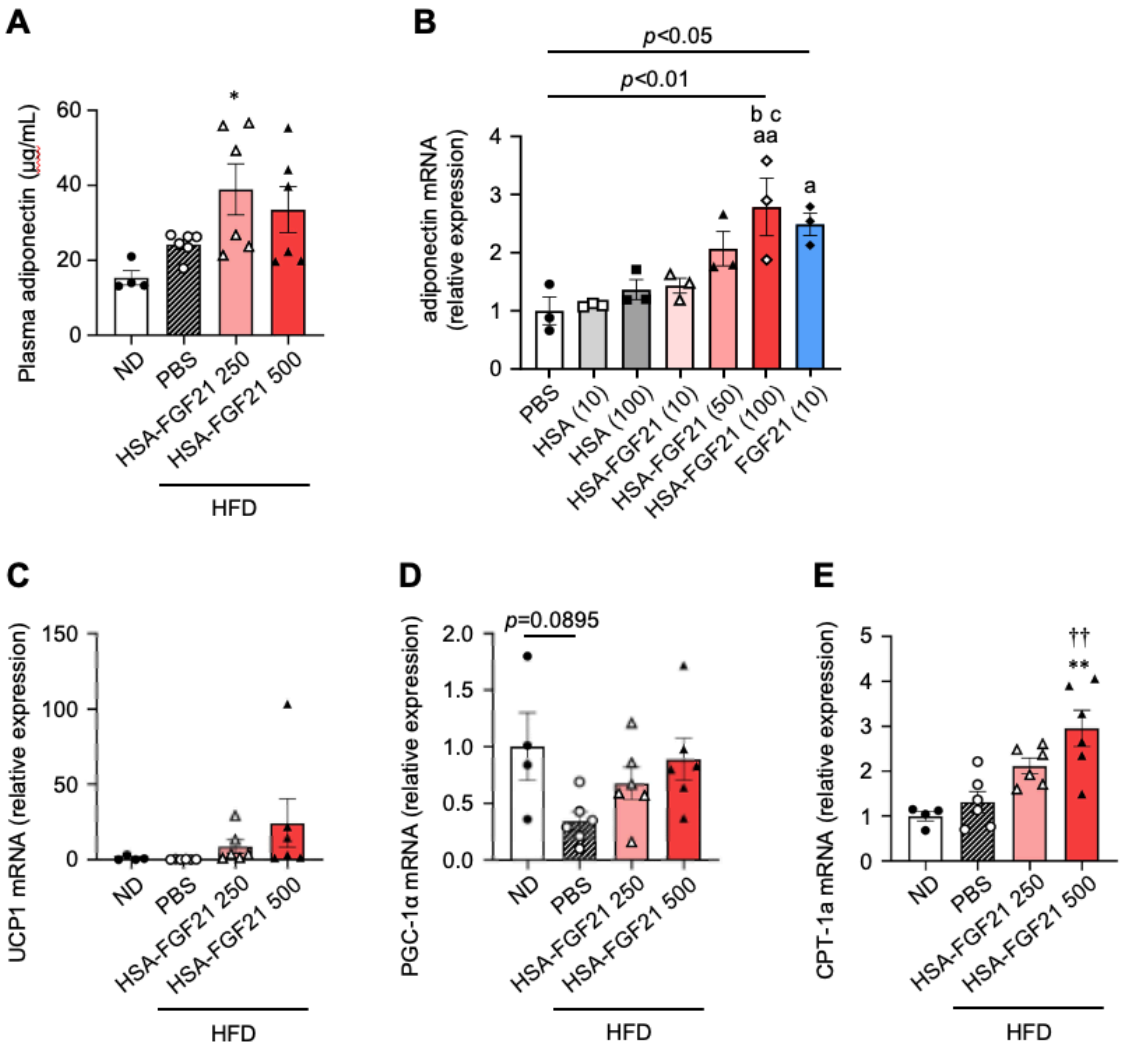

Figure 5. Effect of HSA-FGF21 on adipose tissue

(A) Plasma adiponectin levels were measured at 4 weeks after the administration of HSA-FGF21 in HFD-60-induced model mice (n=4-6). (B) Evaluation of adiponectin-inducing effect of HSA-FGF21 in differentiated 3T3L1 adipocytes. Adiponectin mRNA expression were determined by quantitative RT-PCR (n=3). Results are the mean±S.E. $^{*}p<0.05$ compared with ND group. ap<0.05, aap<0.01 compared with HSA 10 nM, bp<0.05 compared with HSA 100 nM, cp<0.05 compared with HSA-FGF21 10 nM. (C-E) mRNA expression of thermogenic genes (UCP1, PGC-1α, CPT-1a) in ingWAT were determined by quantitative RT-PCR in HFD-60-induced model mice. Results are the means±S.E. (n=4-6). $^{*}p<0.05$, $^{**}p<0.01$ compared with ND group, $^{††}p<0.01$ compared with PBS-treated HFD-60 group.

3.7 Therapeutic effect of HSA-FGF21 on STHD-01-induced NAFLD/NASH model mice

In order to examine the therapeutic effect of HSA-FGF21 in mice with advanced liver damage, we investigated the effect of HSA-FGF21 using high-fat mice that do not develop obesity or abnormal glucose metabolism, but develop liver damage and fibrosis with short-term feeding. The study was conducted using a high-fat and high-cholesterol diet, STHD-01[41]. Early NASH pathology is induced by feeding STHD-01 for 4 weeks[41]. Two weeks after STHD-01 feeding, PBS (10 mL/kg, *iv*) or HSA-FGF21 (500 nmol/kg, *iv*) was administered three times a week for 2 weeks. Telmisartan (5 mg/kg, po) was used as a positive control, based on previous reports, and was administered daily[42](Fig. 6A). Histological evaluation of the liver by Oil Red O staining and HE staining showed that, in the PBS-administered group, large-vesicle lipid droplets and hepatocytes with balloon-like hypertrophy, characteristic indicators of NASH, were observed in a wide area (Fig. 6B and C). The administration of HSA-FGF21 and telmisartan reduced the numbers of lipid droplets and improved lipid accumulation. The amount of TG in the liver increased significantly in the PBS-administered group, while this increase was significantly suppressed in the HSA-FGF21 and telmisartan groups (Fig. 6F). A similar trend was also observed for the amount of TCHO in the liver (Fig. 6G). As a result of measuring plasma ALT and AST, which were elevated as the result of STHD-01 feeding, tended to decrease in the HSA-FGF21 group and the telmisartan group (Fig. 6H, I).

To evaluate oxidative stress in the liver, we performed enzyme immunostaining for nitrotyrosine, a marker for protein oxidative damage. As a result, nitrotyrosine staining was observed mainly around blood vessels in the PBS-administered group, but the intensity of this staining was reduced in the HSA-FGF21 group (Fig. 6D, J). Interestingly, no decrease in nitrotyrosine was observed in the telmisartan group. Regarding inflammation, based on HE staining, multinucleated inflammatory cells was observed, but little such infiltration was observed

in the HSA-FGF21 and telmisartan administration groups (Fig. 6C). Fibrosis is an important prognostic event in the pathology of NASH[43, 44]. Sirius red staining indicated that the accumulation of collagen was observed in the PBS-administered group, but it was suppressed by the administration of HSA-FGF21 (Fig. 6K).

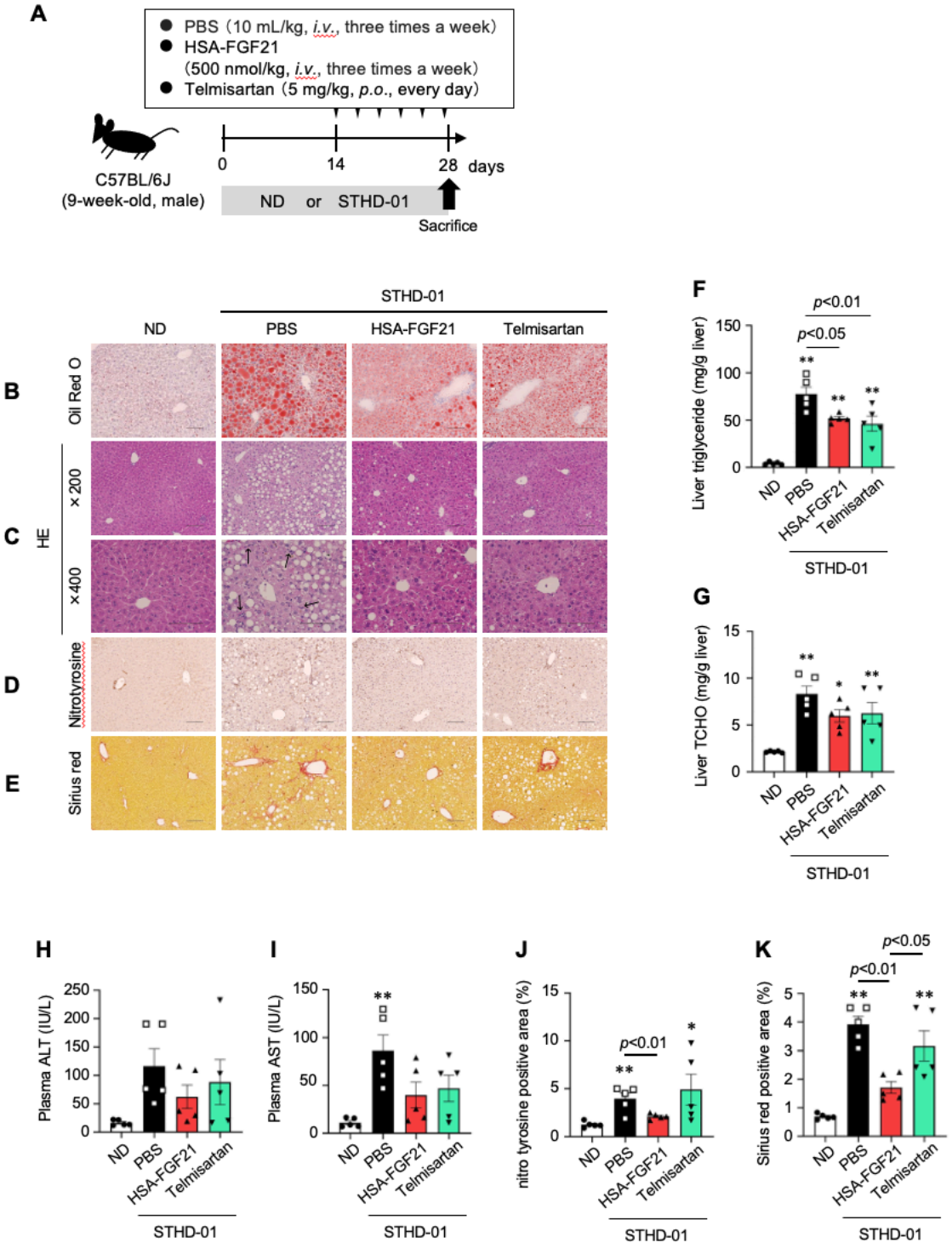
A
PBS (10 mL/kg, i.v., three times a week)
HSA-FGF21
(500 nmol/kg, i.v., three times a week)
Telmisartan (5 mg/kg, p.o., every day)
C57BL/6J
(9-week-old, male)
0
14
28 days
ND or STHD-01
Sacrifice
STHD-01
ND
PBS
HSA-FGF21
Telmisartan
B
Oil Red O
C
HE
× 200
×400
D
Nitrotyrosine
E
Sirius red
F
p<0.01
p<0.05
Liver triglyceride (mg/g liver)
G
Liver TCHO (mg/g liver)
H
Plasma ALT (IU/L)
I
Plasma AST (IU/L)
J
nitro tyrosine positive area (%)
K
Sirius red positive area (%)

Figure 6. Effect of HSA-FGF21 on hepatic steatosis and liver injury in STHD-01-induced NASH model mice

Experimental procedure for evaluating the therapeutic effect of HSA-FGF21 in STHD-01-induced NAFLD/NASH model mice: C57BL/6J mice (9-week-old, male) were fed a ND or STHD-01. Mice were randomized at 14 days after STHD-01 feeding. STHD-01 fed mice were divided into 3 groups: PBS (10 mL/kg, i.v., three times a week), HSA-FGF21 (500 nmol/kg, i.v., three times a week) and telmisartan (5 mg/kg, p.o., everyday) treated group (n=5). Representative photomicrographs of (B) Oil red O, (C) HE, (D) immunohistochemical staining of nitrotyrosine and (E) Sirius red stained liver sections are shown. Original magnification: ×200, 400. Scale bars represent 100 μm. Black arrows indicate inflammatory cells. (F) Hepatic TG and (G) TCHO, plasma (H) ALT and (I) AST levels were measured at 2 weeks after the administration of HSA-FGF21. Quantification of immunohistochemical staining of (J) nitrotyrosine or (K) Sirius red stained area was shown. Results are the means±S.E. (n=5). $^{*}p<0.05$, $^{**}p<0.01$ compared with ND group.

4. Discussion

In recent years, the numbers of NAFLD/NASH patients have been increasing, but there is no effective treatment currently available. Many NAFLD/NASH patients have comorbid obesity and insulin resistance, which are the basis of disease progression. In this study, we prepared a long-acting FGF21 by fusing HSA and mutant FGF21 (HSA-FGF21), and investigated its efficacy against NAFLD/NASH pathology. As a result, HSA-FGF21 exerted a therapeutic effect on hepatic lipid accumulation, obesity and insulin resistance in HFD-60-induced NAFLD model mice. It was revealed that the administration of HSA-FGF21 to STHD-01-induced NAFLD/NASH model mice suppressed the progression of NASH, such as liver damage and fibrosis.

Obesity and insulin resistance are pathological progression factors of NAFLD[1, 6, 45, 46]. In fact, it has been clarified that “improvement of obesity and insulin resistance” in NAFLD model mice is a factor that determines the efficacy of therapeutic drug candidates[47]. In this study, the administration of HSA-FGF21 to HFD-60-induced NAFLD mice simultaneously improved hepatic lipid accumulation, increased body weight and adipose tissue weight, impaired glucose tolerance, and dyslipidemia. These collective findings suggest that HSA-FGF21 could be a new single drug candidate for treating NAFLD pathology.

The effects of HSA-FGF21 in improving NAFLD pathology include five pathways, i.e., 1) suppression of fatty acid uptake into the liver, 2) suppression of excessive fatty acid synthesis, 3) changes in fatty acid composition, 4) the induction of adiponectin and 5) the induction of thermogenesis in adipose tissue (Fig. 7). In particular, the inhibition of hepatic fatty acid uptake and fatty acid synthesis has an effect on the improvement of hepatic lipid accumulation. SREBP-1c, which regulates the expression of CD36 and fatty acid synthase (FAS, SCD-1, Elovl6) is regulated by the nuclear transcription factor liver X receptor (LXR)[48, 49]. Previous reports

showed that feeding HFD activates LXR and increased the expression of SREBP-1c and CD36[50, 51]. Therefore, it was speculated that the suppression of LXR may be involved in the effect of HSA-FGF21. In addition, the hepatic expression of the FGF21 receptor (FGFR1c) is low so that HSA-FGF21 appears to act on adipose tissue in the same manner as FGF21. FGF21 suppressed LXR activity in the liver *via* inducing the production of adiponectin and promoting energy consumption in adipose tissues. Adiponectin activates AMPK in the liver, and AMPK has been reported to suppress the activity of LXR[52-54]. Although AMPK activation was not observed at the time of this study, Bernardo et al. reported that the administration of FGF21 activates AMPK in the liver[55]. Taking these data into consideration, the AMPK/LXR pathway may be involved in the suppression of hepatic SREBP-1c and CD36 expression as the result of the action of HSA-FGF21.

In addition to SREBP-1c, the increased expression of fatty acid synthases such as Elovl6 and SCD-1 was shown to induce insulin resistance in tissues such as the liver and muscle[56, 57] [58]. It is particularly noteworthy that SREBP-1c was shown to induce insulin resistance by suppressing the expression of insulin receptor substrate 2 (IRS-2), which is responsible for insulin signaling. In addition, when insulin resistance occurs, the levels of IRS-1, which mediates lipid synthesis *via* increasing SREBP-1c, was also induced[59, 60]. It therefore appears that HSA-FGF21 could suppress the vicious cycle of insulin resistance and fatty acid synthesis.

In recent years, it has been shown that qualitative changes in fatty acids, such as differences in fatty acid chain length and double bonds, are involved in the homeostasis and pathogenesis of various organs such as the liver and pancreatic β-cells[28, 29]. In fact, in patients with fatty liver and NASH, it was reported that fatty acid composition in the liver changes with the progression of the disease[26]. Consistent with previously reported clinical data, this study showed that C16:0, C18:0, C18:1 and C18:2 fatty acids were increased with HFD-60 feeding. In

the HSA-FGF21 administration group, these increases in C16:0, C18:0, C18:1 and C18:2 were suppressed in all cases, and HSA-FGF21 caused the composition of abnormal fatty acids in the liver became normal. Since saturated fatty acids such as C16:0 or C18:0 induce oxidative stress, ER stress, inflammation and apoptosis, it has been reported that an increase in saturated fatty acids is involved in the development of insulin resistance and NASH[61-63]. On the other hand, unsaturated fatty acids such as C18:1 are less toxic than saturated fatty acids, but are easily taken up by TGs and are involved in cellular lipid accumulation [32]. Therefore, the suppression of C16:0, C18:0 and C18:1 accumulation by HSA-FGF21 appears to be a factor in the improvement of liver damage and hepatic lipid accumulation.

It is very important to consider both *in viv*o pharmacokinetic advantage and *in vitro* activity in the albumin-fusion protein. In this study, FGF21 induced the same level of adiponectin expression as HSA-FGF21 at a concentration of about 1/6 that of HSA-FGF21 in differentiated 3T3L1 adipocytes (Fig. 5B). Previously, it was demonstrated that albumin-interferon-α fusion protein showed higher blood retention and antiviral activity in monkey but approximately 20 times less *in vitro* antiviral activity as compared with non-fused interferon-α[64]. These data suggested that the *in vivo* pharmacokinetic advantage was important even if the *in vitro* activity was less potent.

We previously demonstrated that HSA-FGF21 exerts a hypoglycemic effect at a dose of 500 nmol/kg in studies of the pharmacological effects of HSA-FGF21 on streptozotocin (STZ)-induced type 1 diabetes model mice[24]. In addition, Xu et al. reported that the daily administration of 500 nmol/kg FGF21 improved this pathology after 12 weeks of HFD feeding[15]. In this study, we investigated the pharmacological effects of HSA-FGF21 on HFD-60 or STHD-01-fed mice at doses of 250 nmol/kg and 500 nmol/kg, and found that the administration of 250 nmol/kg three times a week exerted similar disease-improving effects with

that of 500 nmol/kg. In the future, it will be necessary to consider optimizing the dosage and dosing schedule. Currently, several FGF21 products with a higher blood retention such as Fc-fusion or pegylated FGF21 are under development[65]. Based on our previous pharmacokinetic study[24], the adipose tissue distribution of FGF21 might be better in the albumin fusion product compared with Fc-fusion or pegylated FGF21. This study utilized only male mice. It could be important in early-stage pharmacotherapy studies to include both genders in the future.

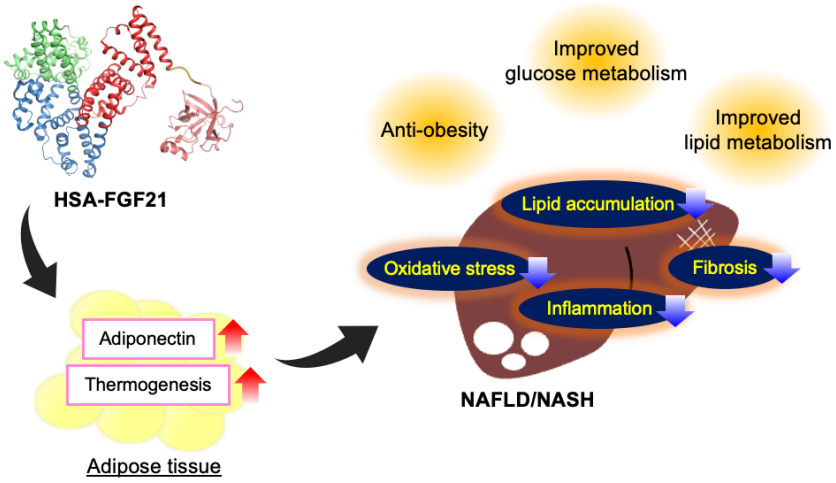

Figure 7. Proposed mechanism responsible for the pharmacological effect of HSA-FGF21 in NAFLD/NASH model mice

5. Conclusion

The findings reported in this study indicate that HSA-FGF21 suppresses hepatic lipid accumulation, improved obesity and insulin resistance, improved adipokine secretion and promoted energy expenditure in high-fat diet-induced NAFLD model mice. In addition, HSA-FGF21 ameliorated the liver damage and fibrosis in early NASH model mice. HSA-FGF21 represents a potentially useful therapeutic agent for the treatment of NAFLD/NASH in the future.

Acknowledgements

This study was funded by the Research Foundation for Pharmaceutical Sciences, a Grant-in-Aid for Scientific Research from the Japan Society for the Promotion of Science (KAKENHI 15H04758; 16H05114), and the Takeda Science Foundation, Japan

Author Contributions

Designed the research studies; Mayuko Chikamatsu, Hiroshi Watanabe

Conducted experiments and acquired data; Mayuko Chikamatsu, Yuhi Shintani, Ryota Murata, Masako Miyahisa, Ayano Nishinoiri, Tadashi Imafuku, Mei Takano, Nanaka Arimura, Kohichi Yamada, Miya Kamimura, Baki Mukai

Contributed new reagents or analytic tools: Takao Satoh

Wrote the manuscript; Mayuko Chikamatsu, Hiroshi Watanabe

Critically reviewed the data and manuscript; Hitoshi Maeda

Supervised the study; Toru Maruyama

Conflict of interest

This study was funded by KM Biologics Co., Ltd.

References

[1] Z. Younossi, F. Tacke, M. Arrese, B. Chander Sharma, I. Mostafa, E. Bugianesi, V. Wai-Sun Wong, Y. Yilmaz, J. George, J. Fan, M.B. Vos, Global Perspectives on Nonalcoholic Fatty Liver Disease and Nonalcoholic Steatohepatitis, Hepatology, 69 (2019) 2672-2682.

[2] C. Estes, H. Razavi, R. Loomba, Z. Younossi, A.J. Sanyal, Modeling the epidemic of nonalcoholic fatty liver disease demonstrates an exponential increase in burden of disease, Hepatology, 67 (2018) 123-133.

[3] D. Kim, A.A. Li, B.J. Perumpail, C. Gadiparthi, W. Kim, G. Cholankeril, J.S. Glenn, S.A. Harrison, Z.M. Younossi, A. Ahmed, Changing Trends in Etiology-Based and Ethnicity-Based Annual Mortality Rates of Cirrhosis and Hepatocellular Carcinoma in the United States, Hepatology, 69 (2019) 1064-1074.

[4] Z.M. Younossi, A.B. Koenig, D. Abdelatif, Y. Fazel, L. Henry, M. Wymer, Global epidemiology of nonalcoholic fatty liver disease-Meta-analytic assessment of prevalence, incidence, and outcomes, Hepatology, 64 (2016) 73-84.

[5] A.E. Reid, Nonalcoholic steatohepatitis, Gastroenterology, 121 (2001) 710-723.

[6] P.T. Campbell, C.C. Newton, N.D. Freedman, J. Koshiol, M.C. Alavanja, L.E. Beane Freeman, J.E. Buring, A.T. Chan, D.Q. Chong, M. Datta, M.M. Gaudet, J.M. Gaziano, E.L. Giovannucci, B.I. Graubard, A.R. Hollenbeck, L. King, I.M. Lee, M.S. Linet, J.R. Palmer, J.L. Petrick, J.N. Poynter, M.P. Purdue, K. Robien, L. Rosenberg, V.V. Sahasrabuddhe, C. Schairer, H.D. Sesso, A.J. Sigurdson, V.L. Stevens, J. Wactawski-Wende, A. Zeleniuch-Jacquotte, A.G. Renehan, K.A. McGlynn, Body Mass Index, Waist Circumference, Diabetes, and Risk of Liver Cancer for U.S. Adults, Cancer Res, 76 (2016) 6076-6083.

[7] T. Tada, H. Toyoda, Y. Sone, S. Yasuda, N. Miyake, T. Kumada, J. Tanaka, Type 2 diabetes mellitus: A risk factor for progression of liver fibrosis in middle-aged patients with non-alcoholic

fatty liver disease, J Gastroenterol Hepatol, 34 (2019) 2011-2018.

[8] H. Jarvis, D. Craig, R. Barker, G. Spiers, D. Stow, Q.M. Anstee, B. Hanratty, Metabolic risk factors and incident advanced liver disease in non-alcoholic fatty liver disease (NAFLD): A systematic review and meta-analysis of population-based observational studies, PLoS Med, 17 (2020) e1003100.

[9] H. Tilg, A.R. Moschen, Evolution of inflammation in nonalcoholic fatty liver disease: the multiple parallel hits hypothesis, Hepatology, 52 (2010) 1836-1846.

[10] X. Zhang, D.C. Yeung, M. Karpisek, D. Stejskal, Z.G. Zhou, F. Liu, R.L. Wong, W.S. Chow, A.W. Tso, K.S. Lam, A. Xu, Serum FGF21 levels are increased in obesity and are independently associated with the metabolic syndrome in humans, Diabetes, 57 (2008) 1246-1253.

[11] A.O. Chavez, M. Molina-Carrion, M.A. Abdul-Ghani, F. Folli, R.A. Defronzo, D. Tripathy, Circulating fibroblast growth factor-21 is elevated in impaired glucose tolerance and type 2 diabetes and correlates with muscle and hepatic insulin resistance, Diabetes Care, 32 (2009) 1542-1546.

[12] D. Barb, F. Bril, S. Kalavalapalli, K. Cusi, Plasma Fibroblast Growth Factor 21 Is Associated With Severity of Nonalcoholic Steatohepatitis in Patients With Obesity and Type 2 Diabetes, J Clin Endocrinol Metab, 104 (2019) 3327-3336.

[13] A. Kharitonenkov, T.L. Shiyanova, A. Koester, A.M. Ford, R. Micanovic, E.J. Galbreath, G.E. Sandusky, L.J. Hammond, J.S. Moyers, R.A. Owens, J. Gromada, J.T. Brozinick, E.D. Hawkins, V.J. Wroblewski, D.S. Li, F. Mehrbod, S.R. Jaskunas, A.B. Shanafelt, FGF-21 as a novel metabolic regulator, J Clin Invest, 115 (2005) 1627-1635.

[14] A. Kharitonenkov, V.J. Wroblewski, A. Koester, Y.F. Chen, C.K. Clutinger, X.T. Tigno, B.C. Hansen, A.B. Shanafelt, G.J. Etgen, The metabolic state of diabetic monkeys is regulated by fibroblast growth factor-21, Endocrinology, 148 (2007) 774-781.

[15] J. Xu, D.J. Lloyd, C. Hale, S. Stanislaus, M. Chen, G. Sivits, S. Vonderfecht, R. Hecht, Y.S. Li, R.A. Lindberg, J.L. Chen, D.Y. Jung, Z. Zhang, H.J. Ko, J.K. Kim, M.M. Véniant, Fibroblast growth factor 21 reverses hepatic steatosis, increases energy expenditure, and improves insulin sensitivity in diet-induced obese mice, Diabetes, 58 (2009) 250-259.

[16] F.M. Fisher, S. Kleiner, N. Douris, E.C. Fox, R.J. Mepani, F. Verdeguer, J. Wu, A. Kharitonenkov, J.S. Flier, E. Maratos-Flier, B.M. Spiegelman, FGF21 regulates PGC-1α and browning of white adipose tissues in adaptive thermogenesis, Genes Dev, 26 (2012) 271-281.

[17] B.M. Owen, X. Ding, D.A. Morgan, K.C. Coate, A.L. Bookout, K. Rahmouni, S.A. Kliewer, D.J. Mangelsdorf, FGF21 acts centrally to induce sympathetic nerve activity, energy expenditure, and weight loss, Cell Metab, 20 (2014) 670-677.

[18] P. Lee, J.D. Linderman, S. Smith, R.J. Brychta, J. Wang, C. Idelson, R.M. Perron, C.D. Werner, G.Q. Phan, U.S. Kammula, E. Kebebew, K. Pacak, K.Y. Chen, F.S. Celi, Irisin and FGF21 are cold-induced endocrine activators of brown fat function in humans, Cell Metab, 19 (2014) 302-309.

[19] Z. Lin, H. Tian, K.S. Lam, S. Lin, R.C. Hoo, M. Konishi, N. Itoh, Y. Wang, S.R. Bornstein, A. Xu, X. Li, Adiponectin mediates the metabolic effects of FGF21 on glucose homeostasis and insulin sensitivity in mice, Cell Metab, 17 (2013) 779-789.

[20] A. Kharitonenkov, J.M. Beals, R. Micanovic, B.A. Strifler, R. Rathnachalam, V.J. Wroblewski, S. Li, A. Koester, A.M. Ford, T. Coskun, J.D. Dunbar, C.C. Cheng, C.C. Frye, T.F. Bumol, D.E. Moller, Rational design of a fibroblast growth factor 21-based clinical candidate, LY2405319, PLoS One, 8 (2013) e58575.

[21] S. Talukdar, Y. Zhou, D. Li, M. Rossulek, J. Dong, V. Somayaji, Y. Weng, R. Clark, A. Lanba, B.M. Owen, M.B. Brenner, J.K. Trimmer, K.E. Gropp, J.R. Chabot, D.M. Erion, T.P. Rolph, B. Goodwin, R.A. Calle, A Long-Acting FGF21 Molecule, PF-05231023, Decreases Body Weight

and Improves Lipid Profile in Non-human Primates and Type 2 Diabetic Subjects, Cell Metab, 23 (2016) 427-440.

[22] X. Ye, J. Qi, Y. Wu, D. Yu, P. Xu, S. Li, S. Zhu, Q. Wu, G. Ren, D. Li, Comparison of PEGylated FGF-21 with insulin glargine for long-lasting hypoglycaemic effect in db/db mice, Diabetes Metab, 41 (2015) 82-90.

[23] R. Hecht, Y.S. Li, J. Sun, E. Belouski, M. Hall, T. Hager, J. Yie, W. Wang, D. Winters, S. Smith, C. Spahr, L.T. Tam, Z. Shen, S. Stanislaus, N. Chinookoswong, Y. Lau, A. Sickmier, M.L. Michaels, T. Boone, M.M. Véniant, J. Xu, Rationale-Based Engineering of a Potent Long-Acting FGF21 Analog for the Treatment of Type 2 Diabetes, PLoS One, 7 (2012) e49345.

[24] H. Watanabe, M. Miyahisa, M. Chikamatsu, K. Nishida, Y. Minayoshi, M. Takano, S. Ichimizu, Y. Kobashigawa, H. Morioka, H. Maeda, T. Maruyama, Development of a long acting FGF21 analogue-albumin fusion protein and its anti-diabetic effects, J Control Release, 324 (2020) 522-531.

[25] T. Imafuku, H. Watanabe, T. Satoh, T. Matsuzaka, T. Inazumi, H. Kato, S. Tanaka, Y. Nakamura, T. Nakano, K. Tokumaru, H. Maeda, A. Mukunoki, T. Takeo, N. Nakagata, M. Tanaka, K. Matsushita, S. Tsuchiya, Y. Sugimoto, H. Shimano, M. Fukagawa, T. Maruyama, Advanced Oxidation Protein Products Contribute to Renal Tubulopathy, Kidney360, 1 (2020) 781-796.

[26] K. Yamada, E. Mizukoshi, H. Sunagozaka, K. Arai, T. Yamashita, Y. Takeshita, H. Misu, T. Takamura, S. Kitamura, Y. Zen, Y. Nakanuma, M. Honda, S. Kaneko, Characteristics of hepatic fatty acid compositions in patients with nonalcoholic steatohepatitis, Liver Int, 35 (2015) 582-590.

[27] T. Matsuzaka, H. Shimano, N. Yahagi, T. Kato, A. Atsumi, T. Yamamoto, N. Inoue, M. Ishikawa, S. Okada, N. Ishigaki, H. Iwasaki, Y. Iwasaki, T. Karasawa, S. Kumadaki, T. Matsui, M. Sekiya, K. Ohashi, A.H. Hasty, Y. Nakagawa, A. Takahashi, H. Suzuki, S. Yatoh, H. Sone, H.

Toyoshima, J. Osuga, N. Yamada, Crucial role of a long-chain fatty acid elongase, Elovl6, in obesity-induced insulin resistance, Nat Med, 13 (2007) 1193-1202.

[28] T. Matsuzaka, A. Atsumi, R. Matsumori, T. Nie, H. Shinozaki, N. Suzuki-Kemuriyama, M. Kuba, Y. Nakagawa, K. Ishii, M. Shimada, K. Kobayashi, S. Yatoh, A. Takahashi, K. Takekoshi, H. Sone, N. Yahagi, H. Suzuki, S. Murata, M. Nakamuta, N. Yamada, H. Shimano, Elovl6 promotes nonalcoholic steatohepatitis, Hepatology, 56 (2012) 2199-2208.

[29] H. Zhao, T. Matsuzaka, Y. Nakano, K. Motomura, N. Tang, T. Yokoo, Y. Okajima, S.I. Han, Y. Takeuchi, Y. Aita, H. Iwasaki, S. Yatoh, H. Suzuki, M. Sekiya, N. Yahagi, Y. Nakagawa, H. Sone, N. Yamada, H. Shimano, Elovl6 Deficiency Improves Glycemic Control in Diabetic, Diabetes, 66 (2017) 1833-1846.

[30] M. Ricchi, M.R. Odoardi, L. Carulli, C. Anzivino, S. Ballestri, A. Pinetti, L.I. Fantoni, F. Marra, M. Bertolotti, S. Banni, A. Lonardo, N. Carulli, P. Loria, Differential effect of oleic and palmitic acid on lipid accumulation and apoptosis in cultured hepatocytes, J Gastroenterol Hepatol, 24 (2009) 830-840.

[31] S.L. Friedman, B.A. Neuschwander-Tetri, M. Rinella, A.J. Sanyal, Mechanisms of NAFLD development and therapeutic strategies, Nat Med, 24 (2018) 908-922.

[32] L.L. Listenberger, X. Han, S.E. Lewis, S. Cases, R.V. Farese, D.S. Ory, J.E. Schaffer, Triglyceride accumulation protects against fatty acid-induced lipotoxicity, Proc Natl Acad Sci U S A, 100 (2003) 3077-3082.

[33] D.H. Ipsen, J. Lykkesfeldt, P. Tveden-Nyborg, Molecular mechanisms of hepatic lipid accumulation in non-alcoholic fatty liver disease, Cell Mol Life Sci, 75 (2018) 3313-3327.

[34] K.C. Hames, A. Vella, B.J. Kemp, M.D. Jensen, Free fatty acid uptake in humans with CD36 deficiency, Diabetes, 63 (2014) 3606-3614.

[35] D. Greco, A. Kotronen, J. Westerbacka, O. Puig, P. Arkkila, T. Kiviluoto, S. Laitinen, M.

Kolak, R.M. Fisher, A. Hamsten, P. Auvinen, H. Yki-Järvinen, Gene expression in human NAFLD, Am J Physiol Gastrointest Liver Physiol, 294 (2008) G1281-1287.

[36] S.E. Hughes, Differential expression of the fibroblast growth factor receptor (FGFR) multigene family in normal human adult tissues, J Histochem Cytochem, 45 (1997) 1005-1019.

[37] M.J. Potthoff, T. Inagaki, S. Satapati, X. Ding, T. He, R. Goetz, M. Mohammadi, B.N. Finck, D.J. Mangelsdorf, S.A. Kliewer, S.C. Burgess, FGF21 induces PGC-1alpha and regulates carbohydrate and fatty acid metabolism during the adaptive starvation response, Proc Natl Acad Sci U S A, 106 (2009) 10853-10858.

[38] K. Maeda, K. Okubo, I. Shimomura, K. Mizuno, Y. Matsuzawa, K. Matsubara, Analysis of an expression profile of genes in the human adipose tissue, Gene, 190 (1997) 227-235.

[39] T. Yoneshiro, S. Aita, M. Matsushita, T. Kayahara, T. Kameya, Y. Kawai, T. Iwanaga, M. Saito, Recruited brown adipose tissue as an antiobesity agent in humans, J Clin Invest, 123 (2013) 3404-3408.

[40] K. Shinoda, K. Ohyama, Y. Hasegawa, H.Y. Chang, M. Ogura, A. Sato, H. Hong, T. Hosono, L.Z. Sharp, D.W. Scheel, M. Graham, Y. Ishihama, S. Kajimura, Phosphoproteomics Identifies CK2 as a Negative Regulator of Beige Adipocyte Thermogenesis and Energy Expenditure, Cell Metab, 22 (2015) 997-1008.

[41] C. Ejima, H. Kuroda, S. Ishizaki, A novel diet-induced murine model of steatohepatitis with fibrosis for screening and evaluation of drug candidates for nonalcoholic steatohepatitis, Physiol Rep, 4 (2016).

[42] J.G. Park, J.S. Mok, Y.I. Han, T.S. Park, K.W. Kang, C.S. Choi, H.D. Park, J. Park, Connectivity mapping of angiotensin-PPAR interactions involved in the amelioration of non-alcoholic steatohepatitis by Telmisartan, Sci Rep, 9 (2019) 4003.

[43] P.S. Dulai, S. Singh, J. Patel, M. Soni, L.J. Prokop, Z. Younossi, G. Sebastiani, M. Ekstedt,

H. Hagstrom, P. Nasr, P. Stal, V.W. Wong, S. Kechagias, R. Hultcrantz, R. Loomba, Increased risk of mortality by fibrosis stage in nonalcoholic fatty liver disease: Systematic review and meta-analysis, Hepatology, 65 (2017) 1557-1565.

[44] H. Hagström, P. Nasr, M. Ekstedt, U. Hammar, P. Stål, R. Hultcrantz, S. Kechagias, Fibrosis stage but not NASH predicts mortality and time to development of severe liver disease in biopsy-proven NAFLD, J Hepatol, 67 (2017) 1265-1273.

[45] J.C. Leung, T.C. Loong, J.L. Wei, G.L. Wong, A.W. Chan, P.C. Choi, S.S. Shu, A.M. Chim, H.L. Chan, V.W. Wong, Histological severity and clinical outcomes of nonalcoholic fatty liver disease in nonobese patients, Hepatology, 65 (2017) 54-64.

[46] S.A. Polyzos, J. Kountouras, C.S. Mantzoros, Obesity and nonalcoholic fatty liver disease: From pathophysiology to therapeutics, Metabolism, 92 (2019) 82-97.

[47] H. Hunter, D. de Gracia Hahn, A. Duret, Y.R. Im, Q. Cheah, J. Dong, M. Fairey, C. Hjalmarsson, A. Li, H.K. Lim, L. McKeown, C.G. Mitrofan, R. Rao, M. Utukuri, I.A. Rowe, J.P. Mann, Weight loss, insulin resistance, and study design confound results in a meta-analysis of animal models of fatty liver, Elife, 9 (2020).

[48] J.J. Repa, G. Liang, J. Ou, Y. Bashmakov, J.M. Lobaccaro, I. Shimomura, B. Shan, M.S. Brown, J.L. Goldstein, D.J. Mangelsdorf, Regulation of mouse sterol regulatory element-binding protein-1c gene (SREBP-1c) by oxysterol receptors, LXRalpha and LXRbeta, Genes Dev, 14 (2000) 2819-2830.

[49] J. Zhou, M. Febbraio, T. Wada, Y. Zhai, R. Kuruba, J. He, J.H. Lee, S. Khadem, S. Ren, S. Li, R.L. Silverstein, W. Xie, Hepatic fatty acid transporter Cd36 is a common target of LXR, PXR, and PPARgamma in promoting steatosis, Gastroenterology, 134 (2008) 556-567.

[50] C. Yan, Y. Zhang, X. Zhang, J. Aa, G. Wang, Y. Xie, Curcumin regulates endogenous and exogenous metabolism via Nrf2-FXR-LXR pathway in NAFLD mice, Biomed Pharmacother,

105 (2018) 274-281.

[51] G. Musso, R. Gambino, M. Cassader, Cholesterol metabolism and the pathogenesis of non-alcoholic steatohepatitis, Prog Lipid Res, 52 (2013) 175-191.

[52] T. Yamauchi, J. Kamon, Y. Minokoshi, Y. Ito, H. Waki, S. Uchida, S. Yamashita, M. Noda, S. Kita, K. Ueki, K. Eto, Y. Akanuma, P. Froguel, F. Foufelle, P. Ferre, D. Carling, S. Kimura, R. Nagai, B.B. Kahn, T. Kadowaki, Adiponectin stimulates glucose utilization and fatty-acid oxidation by activating AMP-activated protein kinase, Nat Med, 8 (2002) 1288-1295.

[53] J. Yang, L. Craddock, S. Hong, Z.M. Liu, AMP-activated protein kinase suppresses LXR-dependent sterol regulatory element-binding protein-1c transcription in rat hepatoma McA-RH7777 cells, J Cell Biochem, 106 (2009) 414-426.

[54] F. Yap, L. Craddock, J. Yang, Mechanism of AMPK suppression of LXR-dependent Srebp-1c transcription, Int J Biol Sci, 7 (2011) 645-650.

[55] B. Bernardo, M. Lu, G. Bandyopadhyay, P. Li, Y. Zhou, J. Huang, N. Levin, E.M. Tomas, R.A. Calle, D.M. Erion, T.P. Rolph, M. Brenner, S. Talukdar, FGF21 does not require interscapular brown adipose tissue and improves liver metabolic profile in animal models of obesity and insulin-resistance, Sci Rep, 5 (2015) 11382.

[56] T. Ide, H. Shimano, N. Yahagi, T. Matsuzaka, M. Nakakuki, T. Yamamoto, Y. Nakagawa, A. Takahashi, H. Suzuki, H. Sone, H. Toyoshima, A. Fukamizu, N. Yamada, SREBPs suppress IRS-2-mediated insulin signalling in the liver, Nat Cell Biol, 6 (2004) 351-357.

[57] T. Matsuzaka, M. Kuba, S. Koyasu, Y. Yamamoto, K. Motomura, S. Arulmozhiraja, H. Ohno, R. Sharma, T. Shimura, Y. Okajima, S.I. Han, Y. Aita, Y. Mizunoe, Y. Osaki, H. Iwasaki, S. Yatoh, H. Suzuki, H. Sone, Y. Takeuchi, N. Yahagi, T. Miyamoto, M. Sekiya, Y. Nakagawa, M. Ema, S. Takahashi, H. Tokiwa, H. Shimano, Hepatocyte ELOVL Fatty Acid Elongase 6 Determines Ceramide Acyl-Chain Length and Hepatic Insulin Sensitivity in Mice, Hepatology, 71 (2020)

1609-1625.

[58] S.M. Rahman, A. Dobrzyn, P. Dobrzyn, S.H. Lee, M. Miyazaki, J.M. Ntambi, Stearoyl-CoA desaturase 1 deficiency elevates insulin-signaling components and down-regulates protein-tyrosine phosphatase 1B in muscle, Proc Natl Acad Sci U S A, 100 (2003) 11110-11115.

[59] M. Kohjima, N. Higuchi, M. Kato, K. Kotoh, T. Yoshimoto, T. Fujino, M. Yada, R. Yada, N. Harada, M. Enjoji, R. Takayanagi, M. Nakamuta, SREBP-1c, regulated by the insulin and AMPK signaling pathways, plays a role in nonalcoholic fatty liver disease, Int J Mol Med, 21 (2008) 507-511.

[60] N. Kubota, T. Kubota, E. Kajiwara, T. Iwamura, H. Kumagai, T. Watanabe, M. Inoue, I. Takamoto, T. Sasako, K. Kumagai, M. Kohjima, M. Nakamuta, M. Moroi, K. Sugi, T. Noda, Y. Terauchi, K. Ueki, T. Kadowaki, Differential hepatic distribution of insulin receptor substrates causes selective insulin resistance in diabetes and obesity, Nat Commun, 7 (2016) 12977.

[61] Y. Wei, D. Wang, F. Topczewski, M.J. Pagliassotti, Saturated fatty acids induce endoplasmic reticulum stress and apoptosis independently of ceramide in liver cells, Am J Physiol Endocrinol Metab, 291 (2006) E275-281.

[62] F. Marra, G. Svegliati-Baroni, Lipotoxicity and the gut-liver axis in NASH pathogenesis, J Hepatol, 68 (2018) 280-295.

[63] S. Fu, S.M. Watkins, G.S. Hotamisligil, The role of endoplasmic reticulum in hepatic lipid homeostasis and stress signaling, Cell Metab, 15 (2012) 623-634.

[64] B.L. Osborn, H.S. Olsen, B. Nardelli, J.H. Murray, J.X. Zhou, A. Garcia, G. Moody, L.S. Zaritskaya, C. Sung, Pharmacokinetic and pharmacodynamic studies of a human serum albumin-interferon-alpha fusion protein in cynomolgus monkeys, J Pharmacol Exp Ther, 303 (2002) 540-548.

[65] C. Degirolamo, C. Sabbà, A. Moschetta, Therapeutic potential of the endocrine fibroblast

growth factors FGF19, FGF21 and FGF23, Nat Rev Drug Discov, 15 (2016) 51-69.

Figure Legends

Figure 1. Effect of HSA-FGF21 on obesity

(A) Experimental procedure for evaluating the therapeutic effect of HSA-FGF21 on HFD-60-induced NAFLD model mice: C57BL/6J mice (4-week-old, male) were fed a normal diet (ND) or high fat diet (HFD-60). Mice were randomized at 12 weeks of HFD-60 feeding, and PBS (10 mL/kg) or HSA-FGF21 (250, 500 nmol/kg) was administered intravenously three times a week for 4 weeks to mice were fed high fat diet (HFD-60). (B) Representative image of mice from each group at 4 weeks after the administration of PBS or HSA-FGF21. (C) Body weight was monitored during the 4 week treatment. **(**D) Representative images of adipose tissues harvested from mice after the treatment. Weight of (E) eWAT, (F) mWAT, (G) ingWAT and (H) iBAT of mice at 4 weeks after the administration of HSA-FGF21. Results are the means±S.E. (n=4-6). $^{*}p<0.05$, $^{**}p<0.01$ compared with ND group, $^{\dagger}p<0.05$, $^{\dagger\dagger}p<0.01$ compared with PBS-treated HFD-60 group.

Figure 2. Effect of HSA-FGF21 on glucose metabolism and dyslipidemia

Fasting (A) blood glucose and (B) plasma insulin levels of mice fasted for 12 hours were measured at day 25 after the administration of HSA-FGF21. (C) OGTT was performed at day 25 after the administration of HSA-FGF21. Mice were fasted for 12 hours prior to an oral administration of D-glucose (2 g/kg). Blood glucose levels were measured at 0, 15, 30, 60 and 120 mins after glucose injection. (D) Plasma triglyceride levels and (E) total cholesterol levels were measured at 4 weeks after the administration of HSA-FGF21. Results are the mean±S.E. (n=4-6). $^{*}p<0.05$, $^{**}p<0.01$ compared with ND group, $^{\dagger}p<0.05$, $^{\dagger\dagger}p<0.01$ compared with PBS-treated HFD-60 group.

Figure 3. Effect of HSA-FGF21 on hepatic steatosis and liver injury

(A) Representative liver tissues that were harvested from mice at 4 weeks after the administration of HSA-FGF21. Representative photomicrographs of hematoxylin and eosin (HE) and Oil red O stained liver sections at 4 weeks after the administration of HSA-FGF21 are shown. Original magnification: ×200. Scale bars represent 100 μm. (B) Liver weight of mice at 4 weeks after the administration of HSA-FGF21. (C) Hepatic TG and (D) TCHO levels were measured at 4 weeks after the administration of HSA-FGF21. Plasma (E) ALT and (F) AST levels were measured at 4 weeks after the administration of HSA-FGF21. Results are the mean±S.E. (n=4-6). $^{**}p<0.01$ compared with ND group, $^{\dagger}p<0.05$, $^{\dagger\dagger}p<0.01$ compared with PBS-treated HFD-60 group.

Figure 4. Effect of HSA-FGF21 on fatty acids composition and genes expression related to hepatic lipid accumulation

(A) Hepatic fatty acid composition was determined using GC-MS at 4 weeks after the administration of HSA-FGF21. (B) Lipid uptake-related gene (CD36) and (C) lipid synthesis-related genes (SREBP-1c, FAS, SCD-1, Elovl6) mRNA expression in liver were determined by quantitative RT-PCR. (D) Western blot analysis of AMPK protein and phosphorylated AMPK in the liver, and (E) fatty acid oxidation-related genes (PPARα, CPT-1a) and (F) lipid efflux-related gene (MTP) mRNA expression in liver were determined at 4 weeks after the administration of HSA-FGF21. Results are the mean±S.E. (n=4-6). $^{*}p<0.05$, $^{**}p<0.01$ compared with ND group, $^{\dagger}p<0.05$, $^{\dagger\dagger}p<0.01$ compared with PBS-treated HFD-60 group.

Figure 5. Effect of HSA-FGF21 on adipose tissue

(A) Plasma adiponectin levels were measured at 4 weeks after the administration of HSA-FGF21 in HFD-60-induced model mice (n=4-6). (B) Evaluation of adiponectin-inducing effect of HSA-FGF21 in differentiated 3T3L1 adipocytes. Adiponectin mRNA expression were determined by

quantitative RT-PCR (n=3). Results are the mean±S.E. $^{*}p<0.05$ compared with ND group. $^{a}p<0.05$, $^{aa}p<0.01$ compared with HSA 10 nM, $^{b}p<0.05$ compared with HSA 100 nM, $^{c}p<0.05$ compared with HSA-FGF21 10 nM. (C-E) mRNA expression of thermogenic genes (UCP1, PGC-1α, CPT-1a) in ingWAT were determined by quantitative RT-PCR in HFD-60-induced model mice. Results are the means±S.E. (n=4-6). $^{*}p<0.05$, $^{**}p<0.01$ compared with ND group, $^{\dagger\dagger}p<0.01$ compared with PBS-treated HFD-60 group.

Figure 6. Effect of HSA-FGF21 on hepatic steatosis and liver injury in STHD-01-induced NASH model mice

Experimental procedure for evaluating the therapeutic effect of HSA-FGF21 in STHD-01-induced NAFLD/NASH model mice: C57BL/6J mice (9-week-old, male) were fed a ND or STHD-01. Mice were randomized at 14 days after STHD-01 feeding. STHD-01 fed mice were divided into 3 groups: PBS (10 mL/kg, *i.v.*, three times a week), HSA-FGF21 (500 nmol/kg, *i.v.*, three times a week) and telmisartan (5 mg/kg, *p.o.*, everyday) treated group (n=5). Representative photomicrographs of (B) Oil red O, (C) HE, (D) immunohistochemical staining of nitrotyrosine and (E) Sirius red stained liver sections are shown. Original magnification: ×200, 400. Scale bars represent 100 μm. Black arrows indicate inflammatory cells. (F) Hepatic TG and (G) TCHO, plasma (H) ALT and (I) AST levels were measured at 2 weeks after the administration of HSA-FGF21. Quantification of immunohistochemical staining of (J) nitrotyrosine or (K) Sirius red stained area was shown. Results are the means±S.E. (n=5). $^{*}p<0.05$, $^{**}p<0.01$ compared with ND group.

Figure 7. Proposed mechanism responsible for the pharmacological effect of HSA-FGF21 in NAFLD/NASH model mice